DOI: 10.1002/ejic.200900652

Synthesis and Characterization of Linear Tetranuclear Silver(I) Complexes Bridged by Tetraphosphane Ligands

Yukie Takemura,[a] Takayuki Nakajima,[a] and Tomoaki Tanase*[a]

Keywords: Silver / Phosphane ligands / Multinuclear complexes / Isocyanide ligands

Reactions of AgOTf with *meso*-bis[(diphenylphosphanylmethyl)phenylphosphanyl]methane (dpmppm) afforded $[Ag_4(OTf)_2(\mu\text{-}OTf)(\mu\text{-dpmppm})_2\{(CH_3)_2CO\}](OTf)$ (**1**) and $[Ag_4(OTf)_2(\mu\text{-}OTf)(\mu\text{-dpmppm})_2(RNC)_2](OTf)$ {R = Xyl (**2a**), Mes (**2b**), *t*Bu (**2c**)}. When AgOTf was treated with dpmppm in air in the presence of *t*BuNC, cleavage of the C–Cl and P–C bonds occurred to give $[Ag_4(\mu\text{-}Cl)(\mu\text{-dpmppm})_2(t\text{BuNC})_4](OTf)_3$ (**3**) and $[Ag_4(\mu\text{-}Ph_2PO_2)(\mu\text{-dpmppm})_2(t\text{BuNC})_3](OTf)_3$ (**4**). Reaction of $AgOCOCF_3$ with dpmppm resulted in $[Ag_4(OCOCF_3)_2(\mu\text{-}OCOCF_3)(\mu\text{-dpmppm})_2](CF_3COO)$ (**5**). By treatment of $AgPF_6$ with dpmppm, $[Ag_4(\mu\text{-dpmppm})_2(t\text{BuNC})_4](PF_6)_4$ (**6**) and $[Ag_4(PO_2F_2)_2(\mu\text{-dpmppm})_2(t\text{BuNC})_2](PF_6)_2$ (**7**) were obtained. Wheareas complexes **1**–**3** possess a $\{Ag_4(\mu\text{-dpmppm})_2\}^{4+}$ core in which the Ag_4 strings are rather bent with two dpmppm ligands arranged in a *syn* fashion, complexes **4**–**7** have linear Ag_4 strings supported by two dpmppm ligands arranged in an *anti* fashion. These results suggest that the dpmppm-supported tetrasilver(I) strings are quite flexible and labile and thus are potentially important in promoting organic reactions as a result of the multimetallic centers.

Introduction

A number of studies on silver(I) complexes have demonstrated the structural diversity induced by the employment of various ligands, counter anions, and solvents.[1,2] In particular, phosphane ligands are shown to influence the geometrical structures of silver(I) centers, from two-coordinate linear structures with bulky phosphanes[3] to four-coordinate tetrahedral with sterically less-hindered phosphanes.[4] Bidentate phosphane ligands are also able to have an effect on dinuclear Ag^I structures, depending on the length of the linker chains between the two phosphorus atoms; diphosphanes with longer methylene chains form the dinuclear complexes $[Ag_2(\mu\text{-}X)_2(\mu\text{-diphosphane})_2]$, in which the silver(I) ions adopt a four-coordinate tetrahedral geometry,[5] and, in contrast, diphosphanes bridged by a methylene or an amide linker give the complexes $[Ag_2(\mu\text{-diphosphane})_2]X_2$ and $[Ag_2X_2(\mu\text{-diphosphane})_2]$, in which the silver(I) ions are located in a two-coordinate linear and a three-coordinate T-shape geometry, respectively.[6] In addition, triangular complexes with a $\{Ag_3(\mu\text{-diphosphane})_3\}^{3+}$ core have also been reported.[7] This flexible coordination behavior of silver(I) ions is regarded as an important factor for their catalytic activities in organic synthesis.[8]

Although di- and multinuclear silver(I) complexes have been synthesized by using bis(diphenylphosphanyl)methane (dppm) and its analogues, linearly ordered polysilver(I) complexes with polydentate phosphanes have largely been unexplored. There is only one characterized example of a linear trinuclear silver(I) complex with a triphosphane supporting ligand, bis(diphenylphosphanylmethyl)phenylphosphane (dpmp), reported by Che and co-workers,[9] whereas a number of homo- and heterotrinuclear complexes with dpmp have been reported by using other transition-metal ions, thus far.[10,11] Recently, we have been successful in preparing a new tetraphosphane ligand, *meso*-bis[(diphenylphosphanylmethyl)phenylphosphanyl]methane (*meso*-1,1,3,5,7,7-hexaphenyl-1,3,5,7-tetraphosphaheptane, abbreviated as dpmppm), in which each phosphorus atom is bridged by a methylene unit. The tetraphosphane dpmppm has proven to be very effective in constructing a bent tetragold(I) chain, as in $[Au_4(\mu\text{-dpmppm})_2]XX'_3$ (X = Cl, X′ = PF_6, BF_4; X = X′ = PF_6),[12] where two dpmppm ligands are disposed in a *syn* arrangement with respect to the Au_4 chain. The flexible tetragold(I) chain shows an interesting fluorescent behavior, which can be switched by capturing a chloride anion, and was further converted into the cyclic hexagold(I) complexes $[Au_6Cl_4(\mu\text{-dpmppm})_2]X_2$ (X = Cl, PF_6) and the linear octagold(I) complex $[Au_8(\mu\text{-}I)_2(\mu_3\text{-}I)_2(\mu\text{-dpmppm})_4](PF_6)_4$. When the copper(I) halide was treated with dpmppm in dichloromethane, ladder-type octanuclear copper(I) complexes $[Cu_8(\mu\text{-}X)_2(\mu_3\text{-}X)_6(\mu\text{-dpmppm})_2]$ (X = Cl, Br, I) were isolated and were readily transformed by treatment with dpmppm in dmso or dmf into the tetracopper(I) complexes containing a bent $\{Cu^I_4(\mu\text{-}X)_3(\mu\text{-dpmppm})_2\}^+$ core.[13]

---

[a] Department of Chemistry, Faculty of Science, Nara Women's University,
Kitauoya-nishi-machi, Nara 630-8506, Japan
Fax: +81-742-20-3399; +81-742-20-3847
E-mail: tanase@cc.nara-wu.ac.jp

In the present study, we have tried to synthesize linear tetrasilver(I) complexes with dpmppm ligands and have revealed that a variety of reactive tetranuclear silver(I) arrays, including those with *syn*- and *anti* arrangements of the two dpmppm ligands, are established according to the type of ancillary ligands as well as counter anions used. In addition to the flexible bent tetranuclear core with two dpmppm ligands arranged in a *syn* fashion as in the Au^I and Cu^I complexes mentioned above, a linear tetrametallic array that is supported by the *anti* arrangement of the two dpmppm ligands is reported in this paper.

Results and Discussion

Synthesis, Structure, and Electrochemical Properties of $[Ag_4(OTf)_2(\mu\text{-}OTf)(\mu\text{-dpmppm})_2\{(CH_3)_2CO\}](OTf)$ (1)

Treatment of AgOTf with dpmppm (2:1 molar ratio) in a CH_2Cl_2/acetone mixed solvent afforded an air-stable, linear tetrasilver(I) complex $[Ag_4(OTf)_2(\mu\text{-}OTf)(\mu\text{-dpmppm})_2\{(CH_3)_2CO\}](OTf)$ (**1**) in 60% yield (Scheme 1). The IR spectrum shows an intense S=O stretching vibration at 1157 cm^{-1}, which indicates the presence of triflate anions. The $^{31}P\{^1H\}$ NMR spectrum of **1** in CD_2Cl_2 consists of two broad multiplets at 13.8 and 9.4 ppm resulting from $^1J_{AgP}$ (≈530 Hz) and $^2J_{PP}$ couplings. The MS (ESI) spectrum in dichloromethane shows a monocation parent peak for $\{Ag_4(OTf)_3(dpmppm)_2\}^+$ at m/z = 2134.903. These results demonstrate that the tetrasilver(I) string of **1** is stable in solution, tentatively as a symmetrical form without acetone coordination.

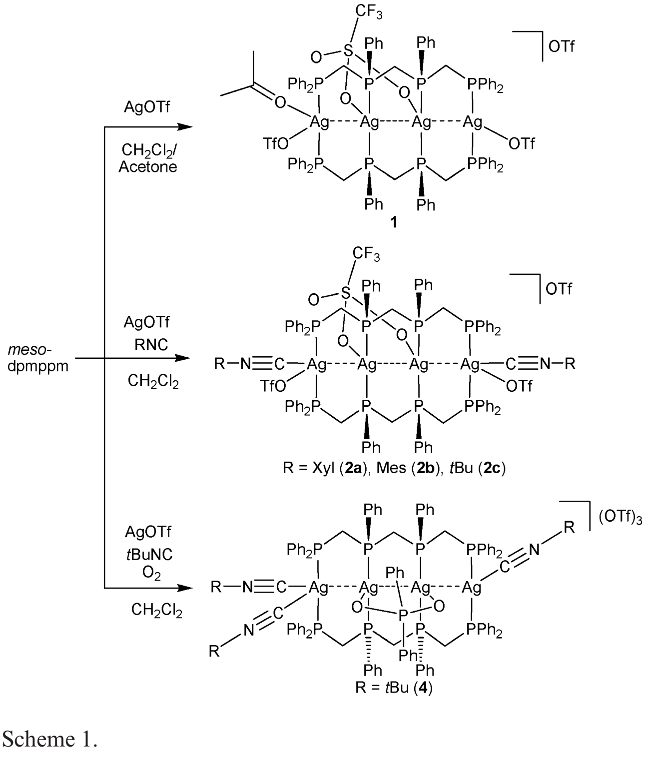

Scheme 1.

The structure of **1** was determined by X-ray crystallographic analysis. The ORTEP plot with the atomic numbering scheme is given in Figure 1, and selected bond lengths and angles are listed in Table 1. The structure consists of a linearly aligned tetrasilver(I) core $\{Ag_4(\mu\text{-dpmppm})_2\}^{4+}$ bridged by two dpmppm ligands. The two dpmppm ligands are arranged in a deformed *syn* orientation (Figure 2) with a pseudo C_2 symmetry around an axis that passes through the Ag2–Ag3 midpoint and the S2 atom. One of the outer silver(I) ions (Ag1) possesses a distorted tetrahedral geometry and is ligated by two P atoms of dpmppm (av. Ag1–P 2.416 Å), one O atom of an acetone molecule [Ag1–O13 2.658(5) Å], and one O atom of a OTf anion [Ag1–O1 2.672(5) Å]. The other outer silver atom (Ag4) is coordinated by two P atoms (av. Ag4–P 2.408 Å) and one O atom of OTf [Ag4–O7 2.593(5) Å comparable to a monodentate OTf anion],[14] which results in a distorted trigonal geometry with the sum of the angles, 359.6°. The inner two silver(I) ions (Ag_{in} = Ag2, Ag3) adopt three-coordinate structures ligated by two P atoms (av. Ag_{in}–P 2.398 Å) and one O atom of a OTf anion with av. Ag_{in}–O 2.757 Å, which is longer than those of monodentate structures. The angles around the Ag2 [90.7(1), 86.0(1), 174.14(5)°] and Ag3 atoms [102.9(1), 79.5(1), 177.54(5)°] indicate that the inner Ag atoms have T-shaped structures. One OTf anion bridges the inner silver(I) ions (O4, O6) and two monodentate OTf anions bond to the outer silver(I) ions (O1, O7) on the opposite side of the Ag_4P_8 plane to the O4 and O6 atoms to form a slightly bent tetrasilver(I) string [Ag1–Ag2–Ag3 156.81(2)°, Ag2–Ag3–Ag4159.30(2)°]. These versatile coordination modes of the OTf^- anion have already been reported.[15] In the previously reported trisilver(I) complex, $[Ag_3(CH_3CN)_2(ClO_4)_2(\mu\text{-dpmp})_2](ClO_4)$ (**8**), two ClO_4^- anions weakly interact with the silver atoms and the trinuclear core is almost linear [175.33(7)°].[9] In silver(I) complexes, there may be argenophilic interactions between the Ag^I ions, although they are weaker than Au···Au aurophilic interactions.[16] The intramolecular Ag···Ag distances of **1** are 3.0125(5) Å (Ag1···Ag2), 3.0419(5) Å (Ag2···Ag3), and 2.9567(5) Å (Ag3···Ag4), which indicates the existence of weak metallophilic interactions in this Ag_4 string.[16] These values are comparable to those found in **8** [2.943(2), 3.014(2) Å].[9] The Ag1···Ag4 distance is 8.598 Å. Complex **1** is the first example of a linear tetrasilver(I) complex supported by polydentate phosphane ligands.

The cyclic voltammogram (CV) of **1** in acetonitrile is shown in Figure 3, together with those for $[Ag_2(OTf)_2(\mu\text{-dppm})_2]$[14a] and $[Ag_3(OTf)_3(\mu\text{-dpmp})_2]$. The CV of **1** shows three irreversible reduction waves at $E_{pc}{}^1$ = –1.79 V, $E_{pc}{}^2$ = –2.16, and $E_{pc}{}^3$ = –2.38 V (vs. Ag/$AgPF_6$). Under the same conditions, the CV of $[Ag_3(OTf)_3(\mu\text{-dpmp})_2]$ shows irreversible reduction waves at $E_{pc}{}^1$ = –1.84 V, $E_{pc}{}^2$ = –2.06, and $E_{pc}{}^3$ = –2.45 V, and that of $[Ag_2(OTf)_2(\mu\text{-dppm})_2]$ at $E_{pc}{}^1$ = –2.09 V. The first reduction peak potentials appreciably shift to higher values on going from the di-, tri-, to the tetrasilver structures. It should be noted that the CV of $[Ag(OTf)(PPh_3)_2]$[17] only shows an intense oxidation peak at around –0.33 V, which is attributable to the decomposed

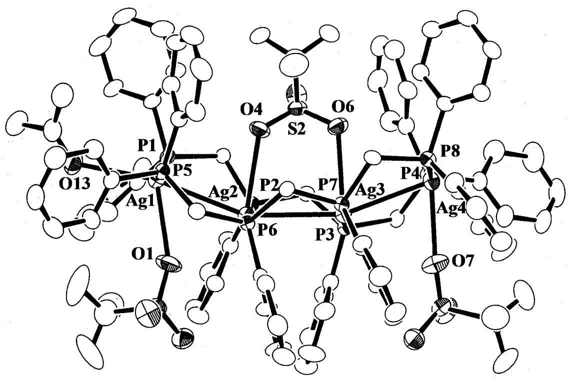

Figure 1. ORTEP plot for the complex cation of **1**, viewed vertical to the Ag_4 chain. The thermal ellipsoids are at the 40% probability level.

Table 1. Selected bond lengths [Å] and angles [°] for complex **1**.[a]

Ag1–O1	2.672(5)	Ag1–O13	2.658(5)
Ag1–P1	2.414(2)	Ag1–P5	2.418(2)
Ag2–O4	2.756(4)	Ag2–P2	2.399(2)
Ag2–P6	2.407(2)	Ag3–O6	2.757(4)
Ag3–P3	2.390(2)	Ag3–P7	2.394(2)
Ag4–O7	2.593(5)	Ag4–P4	2.411(2)
Ag4–P8	2.405(2)	Ag1···Ag2	3.0125(5)
Ag2···Ag3	3.0419(5)	Ag3···Ag4	2.9567(5)
O1–Ag1–O13	110.3(2)	O1–Ag1–P1	113.5(1)
O1–Ag1–P5	87.4(1)	O13–Ag1–P1	87.6(1)
O13–Ag1–P5	100.5(1)	P1–Ag1–P5	153.55(5)
O4–Ag2–P2	90.7(1)	O4–Ag2–P6	86.0(1)
P2–Ag2–P6	174.14(5)	O6–Ag3–P3	102.9(1)
O6–Ag3–P7	79.5(1)	P3–Ag3–P7	177.54(5)
O7–Ag4–P4	92.0(1)	O7–Ag4–P8	108.7(1)
P4–Ag4–P8	158.91(5)		

[a] Estimated standard deviations are given in parentheses.

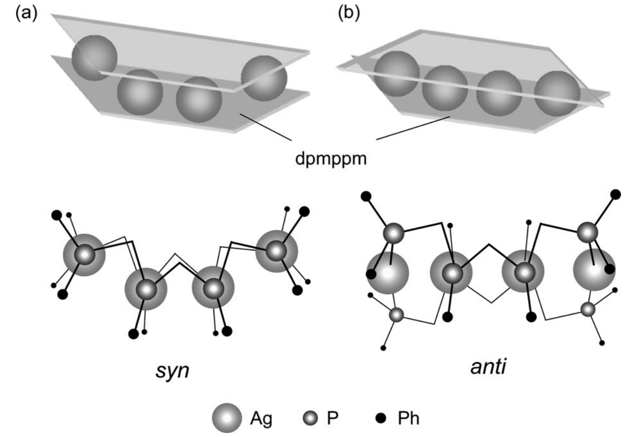

Figure 2. Structures of two dpmppm ligands, which show the Ag_4 string in (a) *syn* and (b) *anti* arrangements.

free Ag^I ions. These results suggest that a reduced species could be stabilized more to some extent in the tetrasilver structure supported by dpmppm ligands, relative to that in the di- and trinuclear silver(I) complexes.

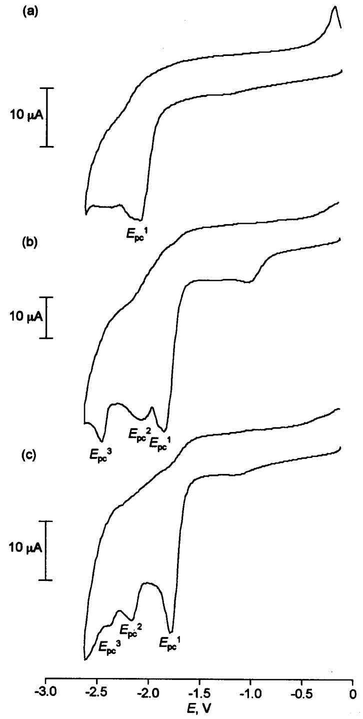

Figure 3. Cyclic voltammograms of (a) $[Ag_2(OTf)_2(\mu\text{-dppm})_2]$, (b) $[Ag_3(OTf)_3(\mu\text{-dpmp})_2]$, and (c) **1** in acetonitrile containing 0.1 M $[nBu_4N][PF_6]$ at a scan rate of 100 mV s^{-1}.

Linear Tetrasilver(I) Complexes with Terminal Isocyanide Ligands

The dinuclear complexes $[Ag_2(\mu\text{-dppm})_2(t\text{BuNC})_2]X_2$ (X = BF_4, ClO_4) and the polymeric compounds $\{[Ag\{\mu\text{-}Ph_2P(CH_2)_mPPh_2\}(t\text{BuNC})_l]BF_4\}_n$ (m = 4–6, l = 1, 2), $\{[Ag_2\{\mu\text{-}Ph_2P(CH_2)_4PPh_2\}_3(t\text{BuNC})_2](BF_4)_2\}_n$, and $\{[Ag\{\mu\text{-}Ph_2P(CH_2)_mPPh_2\}(\mu\text{-dmb})]X\}_n$ (m = 1, 4–6; dmb = 1,8-diisocyano-*p*-menthane; X = BF_4, ClO_4) are known.[18] However, discrete silver(I) complexes that has more than three silver(I) ions with isocyanide ligands have never been reported. To expand this chemistry, we attempted to introduce isocyanide ligands into the $\{Ag_4(\mu\text{-dpmppm})_2\}^{4+}$ core. When dpmppm was treated with 2 equiv. AgOTf in the presence of isocyanides (RNC), linear tetrasilver(I) complexes $[Ag_4(OTf)_3(dpmppm)_2(RNC)_2](OTf)$ [R = Xyl (**2a**), Mes (**2b**), *t*Bu (**2c**)] were obtained in 63–76% yields (Scheme 1). The IR spectra of **2a**–**2c** indicate the presence of terminal isocyanide ligands with N≡C stretching bands at 2164 (**2a**), 2177 (**2b**), and 2190 cm^{-1} (**2c**). In the ^1H NMR spectra, a singlet peak for the methyl protons of the isocyanide ligands are observed at δ = 2.00 ppm (**2a**), 2.26 (*p*-CH_3) and 1.99 ppm (*o*-CH_3) (**2b**), and 1.29 ppm (*t*Bu) (**2c**). The $^{31}P\{^1H\}$ NMR spectra of complex **2a**–**2c** in CD_2Cl_2 exhibit two multiplets in a 1:1 ratio at about 7.9–13.2 ppm, which are considerably broad because of the presence of ^{107}Ag and ^{109}Ag isotopomers.

The detailed structure of complex **2a** was determined by X-ray crystallography; the ORTEP plot for the complex cation is given in Figure 4, and selected bond lengths and angles are listed in Table 2. The complex cation of **2a** has a crystallographically imposed C_2 symmetry and consists of a $\{Ag_4(OTf)_2(\mu\text{-}OTf)(\mu\text{-dpmppm})_2\}^+$ tetranuclear core. The four silver(I) ions are bridged by two dpmppm ligands in a distorted *syn* arrangement (Figure 2) as in **1**, and the inner two silver atoms are further bridged by a triflate anion, which results in a more linear tetrasilver(I) string [Ag1–Ag2–Ag2* 168.48(1)°] than that in **1** (av. 158.06°). Two triflate anions and isocyanide ligands coordinate to the outer Ag^I ions. The inner silver(I) ions (Ag2) adopt a three-coordinate T-shaped structure with two P atoms (av. Ag2–P 2.400 Å) and one O atom of an OTf anion [Ag2–O 2.704(6) Å]. The outer silver(I) ions (Ag1) have a distorted tetrahedral geometry and are coordinated to two P atoms of dpmppm (av. Ag1–P = 2.457 Å), one C atom of XylNC [Ag1–C1 2.269(8) Å], and one O atom of an OTf anion [Ag1–O1 2.581(5) Å]. The $Ag_{out}\cdots Ag_{in}$ [3.1330(9) Å] and $Ag_{in}\cdots Ag_{in}$ [3.086(1) Å] distances are slightly longer than those of **1** [av. 2.9846, 3.0419(5) Å, respectively].

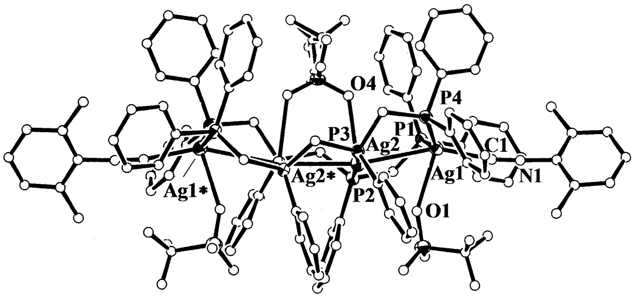

Figure 4. ORTEP plot for the complex cation of **2a**. The Ag, P, and S atoms are drawn with thermal ellipsoids at the 40% probability level, and the other non-hydrogen atoms are shown by circles for clarity.

Table 2. Selected bond lengths [Å] and angles [°] for complex **2a**.[a]

Ag1–C1	2.269(8)	Ag1–O1	2.581(5)
Ag1–P1	2.470(2)	Ag1–P4	2.444(2)
Ag2–O4	2.704(6)	Ag2–P2	2.401(2)
Ag2–P3	2.398(2)	C1–N1	1.12(1)
Ag1···Ag2	3.1330(9)	Ag2···Ag2*	3.086(1)
C1–Ag1–O1	96.2(2)	C1–Ag1–P1	105.2(2)
C1–Ag1–P4	104.1(2)	O1–Ag1–P1	86.6(1)
O1–Ag1–P4	121.1(1)	P1–Ag1–P4	136.51(6)
O4–Ag2–P2	94.4(2)	O4–Ag2–P3	87.0(2)
P2–Ag2–P3	175.35(6)	Ag1–C1–N1	170.7(7)

[a] Estimated standard deviations are given in parentheses.

From the mother liquor of complex **2c**, a very small amount of a chlorido-bridged tetranuclear silver(I) complex $[Ag_4(\mu\text{-}Cl)(\mu\text{-dpmppm})_2(t\text{BuNC})_4](OTf)_3$ (**3**) was obtained (Scheme 2), which suggests that C–Cl bond cleavage of the dichloromethane used as solvent occurs to a small extent during the reaction.

Further, reaction of dpmppm with 2 equiv. AgOTf and excess *t*BuNC in air afforded a tetranuclear silver(I) complex $[Ag_4(\mu\text{-}Ph_2PO_2)(\mu\text{-dpmppm})_2(t\text{BuNC})_3](OTf)_3$ (**4**) in 51% yield (Scheme 1). The structure interestingly involves a phosphinate bridging ligand $Ph_2PO_2^-$, which implies that oxidation of phosphane, followed by P–C bond cleavage of dpmppm, proceeds during the reaction under mild conditions, although the mechanism is not clear. Phosphanes are, in general, stable enough against P–C bond cleavage, and studies on oxidative cleavage of the P–C bond are very few.[19]

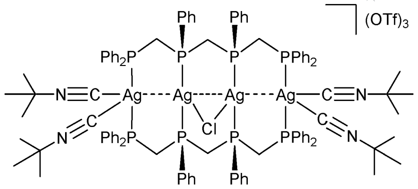

Scheme 2.

The structures of **3** and **4** were determined by X-ray crystallographic analysis. ORTEP plots are given in Figures 5 and 6, and selected bond lengths and angles are listed in Tables 3 and 4, respectively. The structure of **3** consists of a linearly aligned tetrasilver(I) core bridged by two dpmppm ligands with a *syn* arrangement. The inner silver(I) ions (Ag_{in} = Ag2, Ag3) are bridged by a chlorido anion and possess a distorted trigonal geometry by coordination to two P atoms of dpmppm (av. Ag_{in}–P 2.441 Å) and one Cl atom (av. Ag_{in}–Cl1 2.661 Å). Four *t*BuNC ligands bond to the outer Ag^I ions (Ag_{out} = Ag1, Ag4), which have tetrahedral structures with coordination to two P atoms (av. Ag_{out}–P 2.481 Å) and two C atoms of *t*BuNC molecules. While two isocyanide ligands are collinear with the tetrasilver chain and have longer distances (av. Ag–C 2.27 Å), the other two isocyanide ligands are perpendicular to the Ag_4 string and are bent inwards with shorter distances (av. Ag–C 2.22 Å). The tetrasilver string is almost linear, with an av. angle of 172.86°. The structures of **1**, **2a**, and **3** demonstrate that the $Ag_4(\mu\text{-dpmppm})_2$ string is quite flexible, depending on the terminal and bridging ligands. In contrast, the intramolecular Ag···Ag distances of **3** are 3.151 Å (av. $Ag_{in}\cdots Ag_{out}$) and 3.007(1) Å ($Ag_{in}\cdots Ag_{in}$), which are similar to those of **2a** despite the different bridging ligand over the inner Ag atoms.

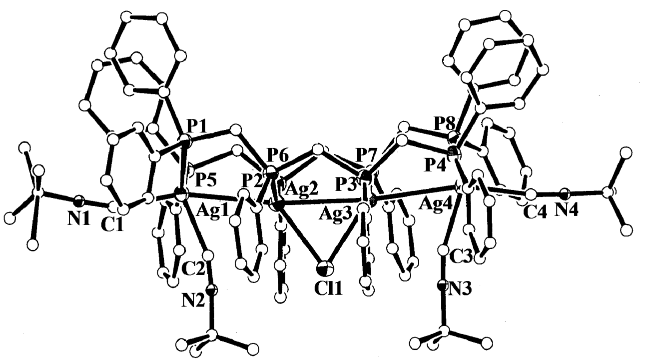

Figure 5. ORTEP plot for the complex cation of **3**. The Ag and P atoms are drawn with thermal ellipsoids at the 40% probability level, and the other non-hydrogen atoms are shown by circles for clarity.

The structure of **4** comprises a dpmppm-bridged tetrasilver(I) core $\{Ag_4(\mu\text{-dpmppm})_2\}^{4+}$ as in **1**, **2a**, and **3**; however, the two dpmppm ligands are in an *anti* arrangement

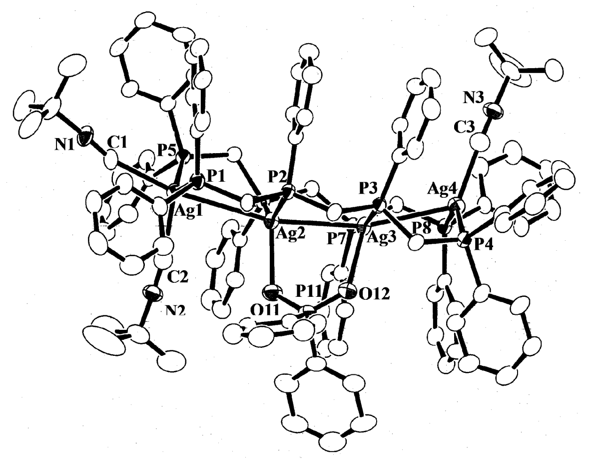

Figure 6. ORTEP plot of the complex cation of **4**. The thermal ellipsoids are drawn at the 40% probability level.

Table 3. Selected bond lengths [Å] and angles [°] for complex **3**.[a]

Ag1–C1	2.26(1)	Ag1–C2	2.232(9)
Ag1–P1	2.478(2)	Ag1–P5	2.476(2)
Ag2–Cl1	2.666(2)	Ag2–P2	2.438(2)
Ag2–P6	2.448(2)	Ag3–Cl1	2.656(2)
Ag3–P3	2.439(2)	Ag3–P7	2.439(2)
Ag4–C3	2.213(10)	Ag4–C4	2.28(1)
Ag4–P4	2.494(2)	Ag4–P8	2.476(2)
C1–N1	1.16(2)	C2–N2	1.14(1)
C3–N3	1.15(1)	C4–N4	1.14(2)
Ag1···Ag2	3.138(1)	Ag2···Ag3	3.007(1)
Ag3···Ag4	3.164(1)		
C1–Ag1–C2	101.3(4)	C1–Ag1–P1	96.5(3)
C1–Ag1–P5	102.5(3)	C2–Ag1–P1	119.7(2)
C2–Ag1–P5	113.3(2)	P1–Ag1–P5	118.09(7)
Cl1–Ag2–P2	110.37(7)	Cl1–Ag2–P6	102.01(7)
P2–Ag2–P6	141.33(7)	Cl1–Ag3–P3	103.87(7)
Cl1–Ag3–P7	108.24(7)	P3–Ag3–P7	141.21(7)
C3–Ag4–C4	99.6(4)	C3–Ag4–P4	114.4(2)
C3–Ag4–P8	120.6(3)	C4–Ag4–P4	105.4(3)
C4–Ag4–P8	96.2(3)	P4–Ag4–P8	115.61(7)
N1–C1–Ag1	158(1)	N2–C2–Ag1	162.8(10)
N3–C3–Ag4	163(1)	N4–C4–Ag4	168.6(9)
Ag2–Cl1–Ag3	68.80(5)		

[a] Estimated standard deviations are given in parentheses.

Table 4. Selected bond lengths [Å] and angles [°] for complex **4**.[a]

Ag1–C1	2.344(2)	Ag1–C2	2.244(2)
Ag1–P1	2.4996(9)	Ag1–P5	2.4921(6)
Ag2–O11	2.322(1)	Ag2–P2	2.436(1)
Ag2–P6	2.4235(7)	Ag3–O12	2.498(2)
Ag3–P3	2.429(1)	Ag3–P7	2.3844(8)
Ag4–C3	2.236(3)	Ag4–P4	2.4662(7)
Ag4–P8	2.477(1)	C1–N1	1.160(2)
C2–N2	1.139(3)	C3–N3	1.140(3)
Ag1···Ag2	3.3193(2)	Ag2···Ag3	3.0371(2)
Ag3···Ag4	3.0867(3)		
C1–Ag1–C2	107.73(8)	C1–Ag1–P1	93.48(7)
C1–Ag1–P5	91.73(7)	C2–Ag1–P1	104.75(8)
C2–Ag1–P5	113.57(7)	P1–Ag1–P5	137.56(2)
O11–Ag2–P2	111.19(5)	O11–Ag2–P6	106.08(5)
P2–Ag2–P6	142.05(2)	O12–Ag3–P3	78.72(4)
O12–Ag3–P7	118.41(4)	P3–Ag3–P7	162.73(2)
C3–Ag4–P4	119.27(8)	C3–Ag4–P8	100.05(8)
P4–Ag4–P8	138.76(2)	N1–C1–Ag1	164.3(2)
N2–C2–Ag1	171.0(2)	N3–C3–Ag4	173.1(2)

[a] Estimated standard deviations are given in parentheses.

with respect to the Ag$_4$ chain (Figure 2) and not in a *syn* arrangement as is usually observed in Au^{I} and Cu^{I} tetranuclear complexes[12,13] and in **1**, **2a**, and **3**. Complex **4** is, thus, the first example of a tetrasilver core in which two dpmppm are in an *anti* arrangement. A phosphinate anion bridges the two inner silver atoms in a μ-η^1:η^1 fashion, and three terminal isocyanide ligands bind to the two outer silver centers, which results in an asymmetrically bent Ag$_4$ string. The average Ag$_3$ angle is 165.55°, which falls in the range between the values of **1** (158.06°) and **2a** [168.48(1)°]. The inner silver(I) ions possess a distorted trigonal geometry by coordination to two P atoms of dpmppm (av. Ag$_{\text{in}}$–P 2.418 Å) and one O atom of the PPh$_2$O$_2^-$ anion (av. Ag$_{\text{in}}$–O 2.41 Å). One of the outer atoms (Ag1) adopts a distorted tetrahedral geometry coordinated by two P atoms (av. Ag1–P 2.4959 Å) and two C atoms of two *t*BuNC molecules (av. Ag1–C 2.294 Å), and the other terminal atom (Ag4) is ligated by two P atoms (av. Ag4–P 2.472 Å) and one C atom of *t*BuNC molecule with a shorter distance 2.236(3) Å. The intramolecular Ag···Ag distances of **4** are 3.3193(2) Å (Ag1···Ag2), 3.0371(2) Å (Ag2···Ag3), and 3.0867(3) Å (Ag3···Ag4).

Synthesis and Structure of [Ag$_4$(OCOCF$_3$)$_2$(μ-OCOCF$_3$)(μ-dpmppm)$_2$](OCOCF$_3$) (5)

Treatment of dpmppm with 2 equiv. AgOCOCF$_3$ in CH$_2$Cl$_2$ afforded an air-stable, linear tetrasilver(I) complex [Ag$_4$(OCOCF$_3$)$_2$(μ-OCOCF$_3$)(μ-dpmppm)$_2$](OCOCF$_3$) (**5**) in 32% yield (Scheme 3). The MS (ESI) spectra show a monocation parent peak for [Ag$_4$(OCOCF$_3$)$_3$(dpmppm)$_2$]$^+$ at m/z = 2027.038, which indicates that the tetrasilver(I) string of **5** is stable in solution.

The detailed structure of **5** was determined by an X-ray crystallographic analysis. The ORTEP plot with the atomic numbering scheme is given in Figure 7, and selected bond lengths and angles are listed in Table 5. The structure consists of a linearly aligned tetrasilver(I) core {Ag$_4$(μ-dpmppm)$_2$}$^{4+}$ bridged by two dpmppm ligands in an *anti* arrangement. A trifluoroacetate anion bridges the inner two Ag atoms in a monodentate fashion, and two additional trifluoroacetate anions coordinate to the outer two Ag atoms on the same side of the Ag$_4$P$_8$ plane. The outer silver(I) ions (Ag1, Ag4) possess a distorted trigonal geometry and are ligated by two P atoms of dpmppm (av. Ag$_{\text{out}}$–P 2.4298 Å) and one O atom of an OTf anion (av. Ag$_{\text{out}}$–O 2.379 Å). The inner silver(I) ions (Ag2, Ag3) are coordinated by two P atoms (av. Ag$_{\text{in}}$–P 2.4096 Å) and bridged by one O atom of OCOCF$_3$ (av. Ag$_{\text{in}}$–O3 2.432 Å), which results in a distorted trigonal geometry. The tetrasilver string is almost linear [Ag1–Ag2–Ag3 168.198(7)°, Ag2–Ag3–Ag4 174.759(6)°], and the intramolecular Ag···Ag distances of **5** are 2.9791(2) Å (Ag1···Ag2), 2.9982(2) Å (Ag2···Ag3), and 2.9884(2) Å (Ag3···Ag4), which are slightly shorter than those of the tetrasilver(I) complexes with triflate anions.

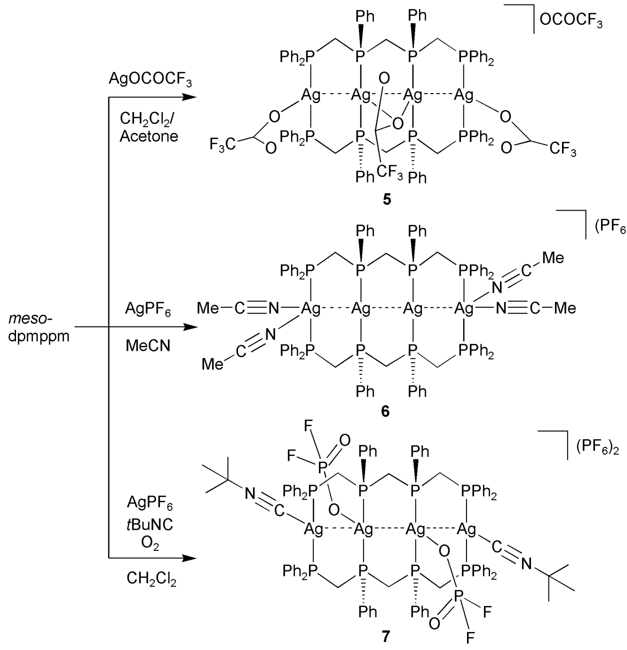

Scheme 3.

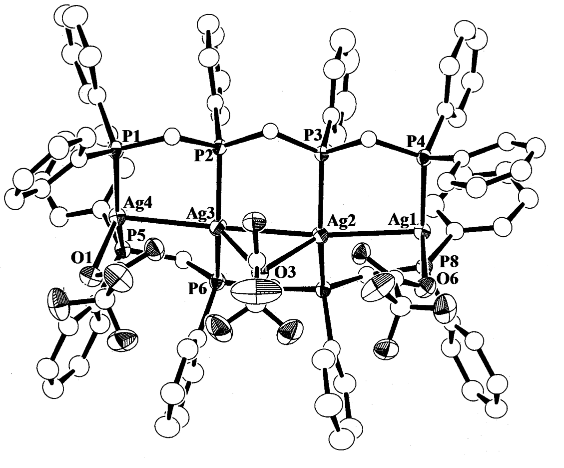

Figure 7. ORTEP plot for the complex cation of **5**. The thermal ellipsoids are drawn at the 40% probability level.

Table 5. Selected bond lengths [Å] and angles [°] for complex **5**.[a]

Ag1–O6	2.363(1)	Ag1–P4	2.4363(3)
Ag1–P8	2.4073(2)	Ag2–O3	2.450(1)
Ag2–P3	2.4176(3)	Ag2–P7	2.4079(2)
Ag3–O3	2.414(1)	Ag3–P2	2.4064(3)
Ag3–P6	2.4064(2)	Ag4–O1	2.395(1)
Ag4–P1	2.4577(4)	Ag4–P5	2.4180(2)
Ag1···Ag2	2.9791(2)	Ag2···Ag3	2.9982(2)
Ag3···Ag4	2.9892(3)		
O6–Ag1–P4	104.06(3)	O6–Ag1–P8	111.89(3)
P4–Ag1–P8	143.77(1)	O3–Ag2–P3	109.61(2)
O3–Ag2–P7	99.50(2)	P3–Ag2–P7	141.46(1)
O3–Ag3–P2	109.90(2)	O3–Ag3–P6	99.77(2)
P2–Ag3–P6	144.94(1)	O1–Ag4–P1	100.75(3)
O1–Ag4–P5	107.88(2)	P1–Ag4–P5	150.60(1)

[a] Estimated standard deviations are given in parentheses.

Reactions of dpmppm with $AgPF_6$

In complexes **1**–**5**, the silver(I) ions weakly interact with the counter anions OTf⁻ and $OCOCF_3^-$. To determine the influence of the anions on the tetrasilver(I) complex, we tried to synthesize a string with a naked $\{Ag_4(\mu\text{-dpmppm})_2\}^{4+}$ core by using the non-coordinating PF_6^- anion. Reaction of dpmppm with $AgPF_6$ and $[Cu(CH_3CN)_4]PF_6$ (1:1:1 molar ratio) in CH_3CN yielded a linear tetrasilver(I) complex $[Ag_4(CH_3CN)_4(\mu\text{-dpmppm})_2](PF_6)_4$ (**6**) in 25% yield (Scheme 3). The IR spectrum of **6** shows the presence of CH_3CN ligands ($\nu_{C\equiv N}$ 2253 cm^{-1}) and PF_6 anions (ν_{PF} 840 cm^{-1}). In the absence of the copper(I) ion, the PF_6^- anion was easily hydrolyzed to afford $PO_2F_2^-$.[5d,19b] Actually, $[Ag_4(\mu\text{-}PO_2F_2)_2(\mu\text{-dpmppm})_2(t\text{BuNC})_2](PF_6)_2$ (**7**) was obtained as crystals in low yield by reacting dpmppm with $AgPF_6$ and *t*BuNC (Scheme 3). The IR spectrum of **7** shows P=O and P–F stretching bands at 1290 and 838 cm^{-1}. The $^{31}P\{^1H\}$ and ^{19}F NMR spectra also indicate the presence of the $PO_2F_2^-$ unit together with PF_6^- anions.

The detailed structures of **6** and **7** were determined by X-ray crystallographic analyses. The ORTEP plots are given in Figures 8 and 9, and selected bond lengths and angles are listed Tables 6 and 7, respectively. The complex cation of **6** has a crystallographically imposed inversion center and is composed of a linearly aligned tetrasilver(I) core $\{Ag_4(\mu\text{-dpmppm})_2\}^{4+}$ bridged by two dpmppm ligands in an *anti* arrangement [Ag1–Ag2–Ag2* 175.84(2)°]. The intramolecular Ag···Ag distances are 3.1014(6) Å (Ag1···Ag2) and 3.0572(5) Å (Ag2···Ag2*). While the outer silver(I) ion (Ag1) possesses a distorted tetrahedral geometry and is ligated by two P atoms of dpmppm (av. Ag1–P 2.4399 Å) and two N atoms of the CH_3CN molecules [Ag1–N1 2.293(16), Ag1–N2 2.534(10) Å], the inner silver atom (Ag2) is coordinated by two P atoms (av. Ag2–P 2.4386 Å), which leads to a linear two-coordinate structure [P2–Ag2–P3 173.08(6)°]. Complex **6** may be potentially important as a catalyst or its precursor and may be useful as a building block, since it involves the naked tetrasilver(I) string surrounded by only labile solvent molecules.

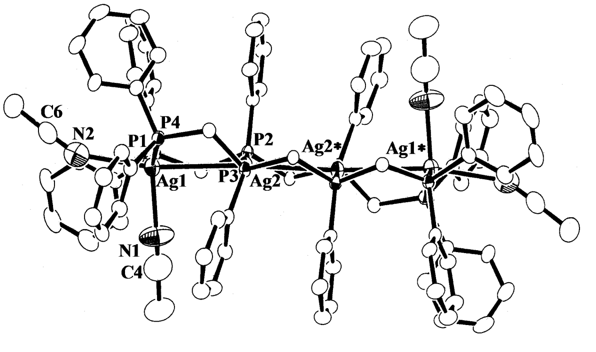

Figure 8. ORTEP plot for the complex cation of **6**. The thermal ellipsoids are drawn at the 40% probability level.

The complex cation of **7** has a crystallographically imposed inversion center and consists of a tetrasilver(I) core $\{Ag_4(\mu\text{-dpmppm})_2\}^{4+}$ bridged by two dpmppm ligands in

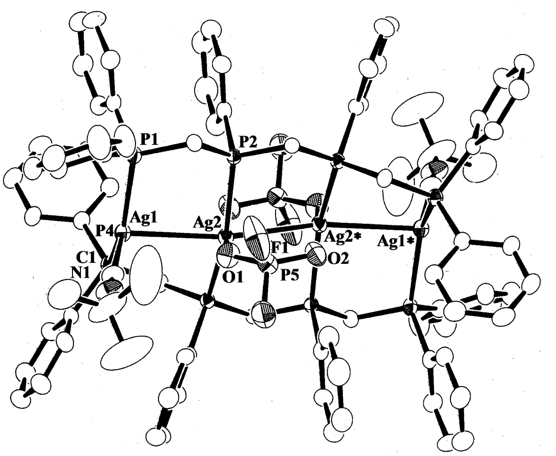

Figure 9. ORTEP plot for the complex cation of **7**. The thermal ellipsoids are drawn at the 40% probability level.

Table 6. Selected bond lengths [Å] and angles [°] for complex **6**.[a]

Ag1–N1	2.293(16)	Ag1–N2	2.534(10)
Ag1–P1	2.4515(15)	Ag1–P4	2.4282(18)
Ag2–P2	2.4370(14)	Ag2–P3	2.4401(15)
C4–N1	1.11(2)	C6–N2	1.20(2)
Ag1···Ag2	3.1014(6)	Ag2···Ag2*	3.0572(2)
N1–Ag1–N2	103.2(4)	N1–Ag1–P1	93.6(3)
N1–Ag1–P4	119.4(3)	N2–Ag1–P1	92.4(2)
N2–Ag1–P4	89.2(2)	P1–Ag1–P4	145.63(6)
P2–Ag2–P3	173.08(6)	C4–N1–Ag1	166.0(12)
C6–N2–Ag1	152.1(8)		

[a] Estimated standard deviations are given in parentheses.

Table 7. Selected bond lengths [Å] and angles [°] for complex **7**.[a]

Ag1–C1	2.218(7)	Ag1–P1	2.475(2)
Ag1–P4	2.436(2)	Ag2–O1	2.425(6)
Ag2–P2	2.412(2)	Ag2–P3	2.382(2)
C1–N1	1.14(1)	Ag1···Ag2	3.0184(6)
Ag1···Ag2*	2.9598(8)		
C1–Ag1–P1	99.0(2)	C1–Ag1–P4	122.4(2)
P1–Ag1–P4	137.51(5)	O1–Ag2–P2	85.2(2)
O1–Ag2–P3	116.5(2)	P2–Ag2–P3	156.96(5)
N1–C1–Ag1	168.8(8)		

[a] Estimated standard deviations are given in parentheses.

an *anti* arrangement. The outer silver(I) ion (Ag1) has a distorted trigonal geometry and is ligated by two P atoms of dpmppm (av. Ag1–P 2.456 Å) and one C atom of *t*BuNC [Ag1–C1 2.218(7) Å], and the inner silver ion (Ag2) adopts a T-shaped structure coordinated by two P atoms (av. Ag2–P 2.397 Å) and one O atom of the PO_2F_2 anion [Ag2–O1 2.425(6) Å]. The intramolecular Ag···Ag distances are 3.0184(6) Å (Ag1···Ag2) and 2.9598(8) Å (Ag2···Ag2*).

Conclusions

In the present study, reactions of *meso*-bis[(diphenylphosphanylmethyl)phenylphosphanyl]methane (dpmppm) with silver(I) salts were systematically investigated to afford a series of tetrasilver(I) complexes in which two dpmppm ligands are arranged in a *syn*- and *anti* fashion. These results suggest that the quite flexible and reactive tetrasilver(I) strings are potentially important in promoting catalytic reactions as a result of the multimetallic centers.

Experimental Section

Materials and General Procedures: All manipulations with the exception of that of **4** were carried out under a nitrogen atmosphere by using standard Schlenk techniques. Bis[(diphenylphosphanylmethyl)phenylphosphanyl]methane (dpmppm),[12] 2,6-xylyl isocyanide (XylNC),[20] and 2,4,6-mesityl isocyanide (MesNC)[20] were prepared by known methods. Reagent grade solvents were dried by standard procedures and were freshly distilled prior to use. IR spectra were recorded on Jasco FT/IR-410 spectrophotometers. ^{1}H, ^{19}F, and $^{31}P\{^{1}H\}$ NMR spectra were recorded on a Varian Gemini 2000 spectrometer at 300, 282, and 121 MHz, respectively. ^{1}H and ^{19}F NMR spectra were referenced to tms and CF_3COOH (–78.45 ppm) as external standards, and $^{31}P\{^{1}H\}$ NMR spectra were referenced to 85% H_3PO_4 as an external standard. MS (ESI-TOF) spectra were recorded on an Applied Biosystems Mariner high-resolution mass spectrometer with positive ionization mode. A Hokuto Denko model HZ-3000 electrochemical analyzer was used in all electrochemical measurements. Tetra-*n*-butylammonium hexafluorophosphate (0.1 M) was used as the supporting electrolyte. Cyclic voltammetry was performed with a conventional electrochemical cell consisting of a glassy carbon working electrode, a $Ag/AgPF_6$ (0.1 M in CH_3CN) reference electrode, and a platinum wire counter electrode. The potential of the $Ag/AgPF_6$ reference electrode was calibrated against the ferrocenium/ferrocene couple before and after each set of experiments to ensure the accuracy of the potential measured; the $E_{1/2}$ of $Cp_2Fe^{+/0}$ was found to be 0.06 ± 0.01 V vs. the $Ag/AgPF_6$ reference.

$[Ag_4(OTf)_3(dpmppm)_2\{(CH_3)_2CO\}](OTf)\cdot CH_2Cl_2$ ($1\cdot CH_2Cl_2$): To a solution of dpmppm (50 mg, 8.0×10^{-2} mmol) in dichloromethane (5 mL) was added AgOTf (41 mg, 0.16 mmol), and the reaction mixture was stirred at room temperature for 12 h. The solution was evaporated to dryness, and the residue was crystallized from an acetone/diethyl ether mixed solvent to afford colorless crystals of $\mathbf{1}\cdot CH_2Cl_2$. Yield: 60% (vs. Ag, 58 mg). $C_{86}H_{80}Ag_4Cl_2F_{12}O_{13}P_8S_4$ (2427.99): calcd. C 42.54, H 3.32, S 5.28; found C 42.65, H 3.37, S 5.62. IR (KBr pellet): $\tilde{\nu}$ = 3057 (m), 1484 (m), 1437 (s), 1370 (m), 1233 (m), 1157 (s), 1102 (m), 1023 (s), 778 (m), 740 (s), 689 (s), 635 (s), 514 (m), 470 (m) cm^{-1}. ^{1}H NMR (300 MHz, CD_2Cl_2, r.t.): δ = 7.64–6.91 (m, 60 H, Ph), 4.03 (br., 2 H, CH_2), 3.79 (br., 8 H, CH_2), 3.04 (br., 2 H, CH_2), 1.78 (br., 6 H, CH_3) ppm. $^{31}P\{^{1}H\}$ NMR (121 MHz, CD_2Cl_2, r.t.): δ = 13.8, 9.4 (dm br., 8 P) ppm. ^{19}F NMR (282 MHz, CD_2Cl_2, r.t.): δ = –78.28 (s, 12 F) ppm. MS (ESI) (CH_2Cl_2): *m/z* = 2134.903 {*z*1, $[Ag_4(OTf)_3(dpmppm)_2]^+$ (2134.831)}.

$[Ag_4(OTf)_3(dpmppm)_2(XylNC)_2](OTf)\cdot CH_2Cl_2$ ($2a\cdot CH_2Cl_2$): To a solution of dpmppm (50 mg, 8.0×10^{-2} mmol) in dichloromethane (7.5 mL) was added AgOTf (40 mg, 0.16 mmol) in the presence of XylNC (78 mg, 0.59 mmol), and the reaction mixture was stirred at room temperature for 12 h to give a pale yellow solution. The solution was concentrated and diethyl ether was slowly added to the solution to afford colorless crystals of $\mathbf{2a}\cdot CH_2Cl_2$. Yield: 76% (vs. Ag, 78 mg). $C_{101}H_{92}Ag_4Cl_2F_{12}N_2O_{12}P_8S_4$ (2632.26): calcd. C 46.09, H 3.52, N 1.06; found C 46.24, H 3.66, N 1.09. IR (KBr pellet): $\tilde{\nu}$ = 3052 (m), 2164 (s), 1484 (m), 1436 (s), 1372 (m), 1236 (s), 1163 (s), 1103 (m), 1024 (s), 776 (m), 739 (s), 690 (s), 635 (s), 514 (m), 471 (m) cm^{-1}. ^{1}H NMR (300 MHz, CD_2Cl_2, r.t.): δ = 7.59–6.87 (m, 66 H, Ph), 4.28 (br., 2 H, CH_2), 3.81 (br., 4 H, CH_2), 3.69 (br., 4 H, CH_2), 2.91 (br., 2 H, CH_2), 2.00 (s, 12 H, CH_3) ppm. $^{31}P\{^1H\}$ NMR (121 MHz, CD_2Cl_2, r.t.): δ = 11.9, 8.0 (m br., 8 P) ppm. ^{19}F NMR (282 MHz, CD_2Cl_2, r.t.): δ = –78.37 (s, 12 F) ppm.

[Ag$_4$(OTf)$_3$(dpmppm)$_2$(MesNC)$_2$](OTf)·0.5CH$_2$Cl$_2$ (2b·0.5CH$_2$Cl$_2$): To a solution of dpmppm (50 mg, 7.9×10^{-2} mmol) in dichloromethane (7.5 mL) was added AgOTf (40 mg, 0.16 mmol) in the presence of MesNC (83 mg, 0.57 mmol), and the reaction mixture was stirred at room temperature for 9 h. The solution was evaporated to dryness. The residue was washed with diethyl ether, extracted with dichloromethane, and crystallized from a dichloromethane/diethyl ether mixed solvent to afford colorless crystals of **2b**·0.5CH$_2$Cl$_2$. Yield: 63% (vs. Ag, 64 mg). $C_{102.5}H_{95}Ag_4ClF_{12}N_2O_{12}P_8S_4$ (2617.85): calcd. C 47.03, H 3.66, N 1.07; found C 47.14, H 3.65, N 1.07. IR (KBr pellet): $\tilde{\nu}$ = 3057 (m), 2177 (m), 1485 (m), 1437 (s), 1375 (m), 1236 (s), 1155 (s), 1097 (m), 1028 (s), 798 (m), 737 (s), 690 (s), 637 (s), 513 (m), 468 (m) cm^{-1}. ^1H NMR (300 MHz, CD_2Cl_2, r.t.): δ = 7.58–6.86 (m, 64 H, Ph), 4.28 (br., 2 H, CH_2), 3.80 (br., 4 H, CH_2), 3.68 (br., 4 H, CH_2), 2.93 (br., 2 H, CH_2), 2.26 (s, 6 H, *p*-CH_3), 1.99 (s, 12 H, *o*-CH_3) ppm. $^{31}P\{^1H\}$ NMR (121 MHz, CD_2Cl_2, r.t.): δ = 11.6, 7.9 (m br., 8 P) ppm.

[Ag$_4$(OTf)$_3$(dpmppm)$_2$(*t*BuNC)$_2$](OTf) (2c): To a solution of dpmppm (51 mg, 8.2×10^{-2} mmol) in dichloromethane (5 mL) was added AgOTf (41 mg, 0.16 mmol) in the presence of *t*BuNC (90 µL, 0.80 mmol), and the reaction mixture was stirred at room temperature for 12 h. The solution was evaporated to dryness. The residue was washed with diethyl ether and was crystallized from a dichloromethane/diethyl ether mixed solvent to afford a white powder of **2c**. Yield: 70% (vs. Ag, 68 mg). $C_{92}H_{90}Ag_4F_{12}N_2O_{12}P_8S_4$ (2451.24): calcd. C 45.08, H 3.70, N 1.14, S 5.23; found C 45.48, H 4.08, N 1.35, S 4.99. IR (KBr pellet): $\tilde{\nu}$ = 3058 (m), 2190 (m), 1484 (m), 1438 (s), 1373 (m), 1230 (s), 1165 (s), 1098 (m), 1030 (s), 796 (m), 742 (s), 691 (s), 636 (s), 515 (m), 473 (m) cm^{-1}. ^1H NMR (300 MHz, CD_2Cl_2, r.t.): δ = 7.46–6.77 (m, 60 H, Ph), 4.25 (br., 2 H, CH_2), 3.76 (br., 4 H, CH_2), 3.64 (br., 4 H, CH_2), 3.08 (br., 2 H, CH_2), 1.29 (s, 18 H, CH_3) ppm. $^{31}P\{^1H\}$ NMR (121 MHz, CD_2Cl_2, r.t.): δ = 13.2–8.0 (m br., 8 P) ppm. ^{19}F NMR (282 MHz, CD_2Cl_2, r.t.): δ = –78.31 (s, 12 F) ppm.

[Ag$_4$Cl(dpmppm)$_2$(*t*BuNC)$_4$](OTf)$_3$ (3): A small amount of crystals of **3** were obtained from the mother liquor of **2c** as mentioned above. The formula was determined by an X-ray crystallographic analysis.

[Ag$_4$(Ph$_2$PO$_2$)(dpmppm)$_2$(*t*BuNC)$_3$](OTf)$_3$·CH$_2$Cl$_2$ (4·CH$_2$Cl$_2$): In air, AgOTf (44 mg, 0.17 mmol) was added to a solution of dpmppm (50 mg, 8.0×10^{-2} mmol) in dichloromethane (3 mL) in the presence of *t*BuNC (90 µL, 0.80 mmol), and the reaction mixture was stirred at room temperature for 12 h. The solution was concentrated, and addition of diethyl ether afforded a white powder of **4**·CH$_2$Cl$_2$. Yield: 51% (vs. Ag, 60 mg). $C_{106}H_{111}Ag_4Cl_2F_9N_3O_{11}P_9S_3$ (2651.39): calcd. C 48.02, H 4.22, N 1.58; found C 48.20, H 4.10, N 1.70. IR (KBr pellet): $\tilde{\nu}$ = 3055 (m), 2174 (m), 1485 (m), 1438 (s), 1374 (m), 1254 (s), 1151 (s), 1098 (m), 1030 (s), 796 (m), 739 (s), 689 (s), 637 (s), 516 (m), 475 (m) cm^{-1}. ^1H NMR (300 MHz, CD_2Cl_2, r.t.): δ = 7.42–6.62 (m, 60 H, Ph), 4.21–3.24 (br., 12 H, CH_2), 1.36 (s, 27 H, CH_3) ppm. $^{31}P\{^1H\}$ NMR (121 MHz, CD_2Cl_2, r.t.): δ = 13.3 ca. –0.5 (m br., 9 P) ppm. ^{19}F NMR (282 MHz, CD_2Cl_2, r.t.): δ = –78.41 (s, 9 F) ppm.

[Ag$_4$(OCOCF$_3$)$_3$(dpmppm)$_2$](OCOCF$_3$)·CH$_2$Cl$_2$ (5·CH$_2$Cl$_2$): To a solution of dpmppm (54 mg, 8.6×10^{-2} mmol) in dichloromethane (5 mL) was added AgOCOCF$_3$ (39 mg, 0.17 mmol), and the reaction mixture was stirred at room temperature for 12 h. The solution was evaporated to dryness, and the residue was crystallized from an acetone/diethyl ether mixed solvent to afford colorless crystals of **5**·CH$_2$Cl$_2$. Yield: 32% (vs. Ag, 31 mg). $C_{87}H_{74}Ag_4Cl_2F_{12}O_8P_8$ (2225.69): calcd. C 46.95, H 3.35; found C 47.08, H 3.34. IR (KBr pellet): $\tilde{\nu}$ = 3055 (m), 1656 (s), 1484 (m), 1437 (s), 1372 (m), 1200 (s), 1133 (s), 1102 (m), 798 (m), 737 (s), 690 (s), 514 (m), 475 (m) cm^{-1}. ^1H NMR (300 MHz, CD_2Cl_2, r.t.): δ = 7.57–6.51 (m, 60 H, Ph), 3.88 (br., 3 H, CH_2), 3.62 (br., 3 H, CH_2), 3.38 (br., 6 H, CH_2) ppm. $^{31}P\{^1H\}$ NMR (121 MHz, CD_2Cl_2, r.t.): δ = 8.25–4.3 (m br., 8 P) ppm. ^{19}F NMR (282 MHz, CD_2Cl_2, r.t.): δ = –74.72 (s, 12 F) ppm. MS (ESI) (CH_2Cl_2): *m*/*z* = 2027.038 {*z*1, [Ag$_4$(CF$_3$CO$_2$)$_3$(dpmppm)$_2$]$^+$ (2026.930)}.

[Ag$_4$(CH$_3$CN)$_4$(dpmppm)$_2$](PF$_6$)$_4$·1.5Et$_2$O (6·1.5Et$_2$O): To a solution of dpmppm (52 mg, 8.3×10^{-2} mmol) in acetonitrile (5 mL) was added AgPF$_6$ (20 mg, 7.8×10^{-2} mmol) in the presence of [Cu(CH$_3$CN)$_4$]PF$_6$ (31 mg, 8.3×10^{-2} mmol), and the reaction mixture was stirred at room temperature for 12 h. The solution was concentrated, and addition of diethyl ether afforded colorless crystals of **6**·1.5Et$_2$O. Yield: 25% (vs. Ag, 13 mg). $C_{92}H_{99}Ag_4F_{24}N_4O_{1.5}P_{12}$ (2543.94): calcd. C 43.44, H 3.92, N 2.20; found C 43.61, H 3.70, N 2.00. IR (KBr pellet): $\tilde{\nu}$ = 3057 (m), 2253 (w), 1485 (m), 1436 (s), 1373 (m), 1101 (m), 840 (s), 793 (m), 739 (s), 688 (s), 557 (m), 474 (m) cm^{-1}. ^1H NMR (300 MHz, CD_2Cl_2, r.t.): δ = 7.59–6.55 (m, 60 H, Ph), 4.00–3.42 (br., 12 H, CH_2), 1.94 (s, 12 H, CH_3) ppm. $^{31}P\{^1H\}$ NMR (121 MHz, CD_2Cl_2, r.t.): δ = 14.8, 10.6 (d br, 4 P) ppm. ^{19}F NMR (282 MHz, CD_2Cl_2, r.t.): δ = –73.58 (d, $^1J_{PF}$ = 709 Hz, 24 F) ppm.

Preparation of [Ag$_4$(PO$_2$F$_2$)$_2$(dpmppm)$_2$(*t*BuNC)$_2$](PF$_6$)$_2$ (7): To a solution of dpmppm (50 mg, 8.0×10^{-2} mmol) in dichloromethane (5 mL) was added AgPF$_6$ (40 mg, 0.16 mmol) in the presence of *t*BuNC (90 µL, 0.80 mmol), and the reaction mixture was stirred at room temperature for 12 h. The solution was concentrated, and addition of diethyl ether afforded colorless crystals of **7**. Yield: 25% (vs. Ag, 24 mg). IR (KBr pellet): $\tilde{\nu}$ = 3055 (m), 2184 (m), 1485 (m), 1436 (s), 1371 (m), 1290 (s), 1130 (s), 1099 (m), 838 (s), 789 (m), 739 (s), 690 (s), 557 (s), 495 (m), 476 (m) cm^{-1}. ^1H NMR (300 MHz, CD_2Cl_2, r.t.): δ = 7.47–6.71 (m, 60 H, Ph), 3.47 (br., 12 H, CH_2), 1.38 (s, 18 H, CH_3) ppm. $^{31}P\{^1H\}$ NMR (121 MHz, CD_2Cl_2, r.t.): δ = 6.6–3.2 (m br., 8 P), –14.0 (t, $^1J_{PF}$ = 973 Hz, 2 P), –144.0 (sept, $^1J_{PF}$ = 712 Hz, 2 P) ppm. ^{19}F NMR (282 MHz, CD_2Cl_2, r.t.): δ = –73.65 (d, $^1J_{PF}$ = 709 Hz, 12 F), –82.05 (d, $^1J_{PF}$ = 969 Hz, 4 F) ppm. Compound **7** was obtained as crystals only in low yield, since unidentified non-hydrolyzed complexes were obtained in the reaction.

Preparation of [Ag$_3$(OTf)$_3$(dpmp)$_2$]: To a solution of dpmp (50 mg, 9.9×10^{-2} mmol) in dichloromethane (2.5 mL) was added AgOTf (38 mg, 15×10^{-2} mmol) in dichloromethane (5 mL), and the reaction mixture was stirred at room temperature for 12 h. The solution was concentrated, and diethyl ether was added to afford microcrystals of [Ag$_3$(OTf)$_3$(dpmp)$_2$]. Yield: 54% (vs. Ag, 47 mg). IR (KBr pellet): $\tilde{\nu}$ = 3057 (m), 1485 (m), 1437 (s), 1371 (w), 1257 (s), 1159 (s), 1101 (m), 1024 (s), 783 (m), 739 (s), 690 (s), 636 (s), 515 (m), 471 (m) cm^{-1}. ^1H NMR (300 MHz, CD_2Cl_2, r.t.): δ = 7.69–7.01 (m, 50 H, Ph), 3.75 (br., 8 H, CH_2) ppm. $^{31}P\{^1H\}$ NMR (121 MHz, CD_2Cl_2, r.t.): δ = 14.2–8.80 (dm br, 6 P) ppm. ^{19}F NMR (282 MHz, CD_2Cl_2, r.t.): δ = –80.07 (s) ppm. MS (ESI) (CH_2Cl_2): *m*/*z* = 1634.754 {*z*1, [Ag$_3$(OTf)$_2$(dpmp)$_2$]$^+$ (1634.916)}.

Preparation of [Ag$_2$(OTf)$_2$(dppm)$_2$]:[14a] To a solution of dppm (100 mg, 26×10^{-2} mmol) in dichloromethane (2.5 mL) was added AgOTf (66 mg, 26×10^{-2} mmol) in dichloromethane (5 mL), and the reaction mixture was stirred at room temperature for 12 h. The solution was concentrated, and diethyl ether was added to give colorless crystals of [Ag$_2$(OTf)$_2$(dppm)$_2$]. Yield: 69% (with respect to Ag, 110 mg). IR (KBr pellet): $\tilde{\nu}$ = 3055 (m), 1485 (m), 1437 (s),

Table 8. Crystallographic data for complexes **1**, **2a**, and **3**–**7**.

	1·$(CH_3)_2CO·2Et_2O$	**2a**	**3**·$CH_2Cl_2·2.5H_2O$	**4**·CH_2Cl_2	**5**·$3CH_2Cl_2·H_2O$	**6**·CH_3CN	**7**·$2CH_2Cl_2·2H_2O$
Empirical formula	$C_{96}H_{104}O_{16}P_8S_4Ag_4F_{16}$	$C_{100}H_{90}N_2O_{12}P_8S_4Ag_4F_{12}$	$C_{102}H_{115}N_4O_{11.5}P_8S_3Ag_4Cl_3F_9$	$C_{109.5}H_{112}N_3O_{11}P_9S_3Ag_4Cl_3F_9$	$C_{89}H_{80}Ag_4Cl_6F_{12}O_9P_8$	$C_{88}H_{87}Ag_4F_{24}N_5P_{12}$	$C_{90}H_{98}Ag_4Cl_4F_{16}N_2O_6P_{12}$
Formula mass	2549.35	2547.30	2633.84	2729.86	2413.57	2473.81	2552.72
Crystal system	monoclinic	orthorhombic	monoclinic	triclinic	triclinic	triclinic	triclinic
Space group	$P2_1/a$	$Pccn$	$P2_1/n$	$P\bar{1}$	$P\bar{1}$	$P\bar{1}$	$P\bar{1}$
a [Å]	27.563(5)	13.3655(5)	21.335(5)	14.750(5)	13.6873(8)	13.780(4)	12.5995(2)
b [Å]	12.477(2)	30.750(1)	22.136(5)	17.396(6)	16.665(1)	13.934(5)	14.6160(1)
c [Å]	33.489(7)	25.240(1)	26.032(6)	25.773(9)	23.106(1)	15.790(6)	17.2136(1)
α [°]				93.315(1)	102.211(2)	89.444(12)	76.07(2)
β [°]	113.084(2)	106.162(1)	101.740(4)	97.424(1)	73.962(8)	69.17(1)	
γ [°]				109.342(4)	107.210(3)	65.806(10)	75.08(1)
V [Å^3]	10594(3)	10373.2(7)	11808(4)	6052(3)	4815.6(5)	2639(2)	2823.6(3)
Z	4	4	4	2	2	1	1
T [°C]	–120	–100	20	–100	–105	–105	–105
D_{calcd} [g cm^{-3}]	1.598	1.631	1.481	1.498	1.664	1.556	1.501
2θ range [°]	6–55	6–55	6–55	6–55	6–55	6–55	6–55
No. unique reflections	24211	11698	26691	27025	21508	11450	12617
No. observations [$I > 2\sigma(I)$]	13889	10970	17400	18853	17239	8005	8909
No. variables	1271	687	1305	1378	1172	615	623
R_1[a]	0.050	0.077	0.097	0.089	0.056	0.094	0.072
wR_2[b]	0.178	0.189	0.297	0.287	0.155	0.322	0.240
GOF	0.72	1.26	0.93	1.02	1.01	1.20	1.09

[a] $R_1 = \Sigma||F_o| - |F_c||/\Sigma|F_o|$ [for reflections with $I > 2\sigma(I)$]. [b] $wR_2 = [\Sigma w(F_o^2 - F_c^2)^2/\Sigma w(F_o^2)^2]^{1/2}$ (for all reflections).

1367 (w), 1238 (s), 1155 (s), 1101 (m), 1024 (s), 741 (s), 692 (s), 636 (s), 515 (s), 474 (m) cm^{-1}. ^{1}H NMR (300 MHz, CD_2Cl_2, r.t.): δ = 7.53–7.31 (m, 40 H, Ph), 3.90 (m, 4 H, CH_2) ppm. ^{31}P{^{1}H} NMR (121 MHz, CD_2Cl_2, r.t.): δ = 12.4, 8.04 (dm br., 4 P) ppm. ^{19}F NMR (282 MHz, CD_2Cl_2, r.t.): δ = –80.02 (s) ppm. MS (ESI) (CH_2Cl_2): m/z = 1132.887 {z1, [Ag_2(OTf)(dppm)$_2$]$^+$ (1133.002)}.

X-ray Crystallography: The crystals of **1**·$(CH_3)_2CO·2Et_2O$, **2a**, **3**·$CH_2Cl_2·2.5H_2O$, **4**·CH_2Cl_2, **5**·$3CH_2Cl_2·H_2O$, **6**·CH_3CN, **7**·$2CH_2Cl_2·2H_2O$ were quickly coated with Paraton N oil and mounted on top of a glass fiber at room temperature. The crystallographic data are summarized in Table 8. All data were collected on a Rigaku AFC8R/Mercury CCD diffractometer equipped with graphite-monochromated Mo-K_α radiation using a rotating-anode X-ray generator. A total of 2160 oscillation images, covering a whole sphere of 6° < 2θ < 55°, were collected with exposure rates of 96 (**2a**), 128 (**3** and **5**–**7**), 192 (**1**), 256 (**4**) s/° by the ω-scan method [–62° < ω < 118°] with a $\Delta\omega$ of 0.25°. The crystal-to-detector (70 × 70 mm) distance was set at 60 mm. The data was processed by using the Crystal Clear 1.3.5 program (Rigaku/MSC) [21] and corrected for Lorentz polarization and absorption effects. The structures of complexes **1**, **2a**, and **3**–**7** were solved by direct methods (DIRDIF94[22] and SIR92/97[23]) and refined on F^2 with full-matrix least-squares techniques with SHELXL97/93[24] by using the teXan and Crystal Structure 3.8 crystallographic software packages.[25,26] In the refinement of **1**, **2a**, and **5**–**7**, all non-H atoms were anisotropically refined, and the C–H hydrogen atoms, except those of disordered solvents, were calculated at ideal positions and were fixed in the refinement. An Et_2O molecule (**1**), the bridging and the counter OTf$^-$ anions (**2a**), an acetonitrile molecule (**6**), and two water molecules (**7**) are disordered. In the refinement of **3** and **4**, all non-H atoms, except the disordered water molecules (**3**) and the disordered C atoms of CH_2Cl_2 (**4**), were refined with anisotropic thermal parameters. In addition to the disordered structures of water (**3**) and dichloromethane (**4**) molecules, one tBu group of the isocyanide ligands in **3** is disordered and refined with a symmetrical model. CCDC-739508 (**1**), -739509 (**2a**), -739510 (**3**), -739511 (**4**), -739512 (**5**), -739513 (**6**), and -739514 (**7**) contain the supplementary crystallographic data for this paper. These data can be obtained free of charge from The Cambridge Crystallographic Data Centre via www.ccdc.cam.ac.uk/data_request/cif.

Acknowledgments

This work was supported by the Grant-in-Aid for Scientific Research from the Ministry of Education, Culture, Sports, Science and Technology of Japan. Y. T. is grateful to the Japan Science Society for generous financial support (Sasakawa Scientific Research Grant) and to the Nara Women's University for a grant for young women researchers.

---

[1] a) G. K. Patra, I. Goldberg, *J. Chem. Soc., Dalton Trans.* **2002**, 1051–1057; b) D. M. L. Goodgame, D. A. Grachvogel, D. J. Williams, *J. Chem. Soc., Dalton Trans.* **2002**, 2259–2260; c) S.-L. Zheng, M.-L. Tong, X.-L. Yu, X.-M. Chen, *J. Chem. Soc., Dalton Trans.* **2001**, 586–592; d) Y. Kang, S. S. Lee, K.-M. Park, S. H. Lee, S. O. Kang, J. Ko, *Inorg. Chem.* **2001**, *40*, 7027–7031; e) W. Su, M. Hong, J. Weng, R. Cao, S. Lu, *Angew. Chem. Int. Ed.* **2000**, *39*, 2911–2914; f) C. B. Aakeröy, A. M. Beatty, *Chem. Commun.* **1998**, 1067–1068; g) L. Carlucci, G. Ciani, D. M. Proserpio, A. Sironi, *J. Am. Chem. Soc.* **1995**, *117*, 4562–4569.

[2] a) M.-C. Brandys, R. J. Puddephatt, *J. Am. Chem. Soc.* **2002**, *124*, 3946–3950; b) F. Bachechi, A. Burini, R. Galassi, B. R. Pietroni, D. Tesei, *Eur. J. Inorg. Chem.* **2002**, 2086–2093; c) M.-C. Brandys, R. J. Puddephatt, *Chem. Commun.* **2001**, 1508–1509; d) E. Lozano, M. Nieuwenhuyzen, S. L. James, *Chem. Eur. J.* **2001**, *7*, 2644–2651.

[3] E. C. Alyea, G. Ferguson, A. Somogyvari, *Inorg. Chem.* **1982**, *21*, 1369–1371.

[4] a) P. F. Barron, J. C. Dyason, P. C. Healy, L. M. Engelhardt, B. W. Skelton, A. H. White, *J. Chem. Soc., Dalton Trans.* **1986**, 1965–1970; b) E. L. Muetterties, C. W. Alegranti, *J. Am. Chem. Soc.* **1972**, *94*, 6386–6391.

[5] a) Effendy, F. Marchetti, C. Pettinari, R. Pettinari, B. W. Skelton, A. H. White, *Inorg. Chim. Acta* **2007**, *360*, 1414–1423; b) Effendy, C. D. Nicola, M. Fianchini, C. Pettinari, B. W. Skelton, N. Somers, A. H. White, *Inorg. Chim. Acta* **2005**, *358*, 763–795; c) F. Caruso, M. Camalli, H. Rimml, L. M. Venanzi, *Inorg. Chem.* **1995**, *34*, 673–679; d) S. Kitagawa, M. Kondo, S. Kawata, S. Wada, M. Maekawa, M. Munakata, *Inorg. Chem.* **1995**, *34*, 1455–1465.

[6] a) H. Krishna, S. S. Krishnamurthy, M. Nethaji, *Polyhedron* **2006**, *25*, 3189–3200; b) Effendy, C. D. Nicola, M. Nitiatmodjo, C. Pettinari, B. W. Skelton, A. H. White, *Inorg. Chim. Acta* **2005**, *358*, 735–747; c) C.-M. Che, M.-C. tse, M. C. W. Chan, K.-K. Cheung, D. L. Phillips, K.-H. Leung, *J. Am. Chem. Soc.* **2000**, *122*, 2464–2468; d) D. Perreault, M. Drouin, A. Michel, V. M. Miskowski, W. P. Schaefer, P. D. Harvey, *Inorg. Chem.* **1992**, *31*, 695–702; e) D. M. Ho, R. Bau, *Inorg. Chem.* **1983**, *22*, 4073–4079.

[7] a) A. A. M. Aley, D. Neugebauer, O. Orama, U. Schubert, H. Schimidbaur, *Angew. Chem. Int. Ed. Engl.* **1978**, *17*, 125–126; b) V. W.-W. Yam, W. K.-M. Fung, K.-K. Cheung, *Chem. Commun.* **1997**, 963–964; c) V. W.-W. Yam, W.-Y. Lo, C.-H. Lam, W. K.-M. Fung, K. M.-C. Wong, V. C.-Y. Lau, N. Zhu, *Coord. Chem. Rev.* **2003**, *245*, 39–47; d) C. D. Nicola, Effendy, F. Fazaroh, C. Pettinari, B. W. Skelton, N. Somers, A. H. White, *Inorg. Chim. Acta* **2005**, *358*, 720–734; e) Q.-H. Wei, G.-Q. Yin, L.-Y. Zhang, Z.-N. Chen, *Inorg. Chem.* **2006**, *45*, 10371–10377; f) H. Krishna, S. S. Krishnamurthy, M. Nethaji, *Polyhedron* **2006**, *25*, 3189–3200.

[8] a) P. J. Pérez, Díaz-Requejo in *Comprehensive Organometallic Chemistry III* (Eds.: R. H. Crabtree, D. M. Mingos), Elsevier Ltd. **2007**, vol. 2, pp. 153–195; b) A. Yanagisawa in *Acid Catalysis in Modern Organic Synthesis* (Eds.: H. Yamamoto, K. Ishihara), Wiley-VCH Verlag GmbH & Co. KGaA, **2008**, vol. 2, pp. 987–1018.

[9] C.-M. Che, H.-K. Yip, D. Li, S.-M. Peng, G.-H. Lee, Y.-M. Wang, S.-T. Liu, *J. Chem. Soc., Chem. Commun.* **1991**, 1615–1617.

[10] a) R. R. Guimerans, M. M. Olmstead, A. L. Balch, *J. Am. Chem. Soc.* **1983**, *105*, 1677–1679; b) M. M. Olmstead, R. R. Guimerans, A. L. Balch, *Inorg. Chem.* **1983**, *22*, 2473–2474; c) A. L. Balch, M. M. Olmstead, R. R. Guimerans, *Inorg. Chim. Acta* **1984**, *84*, L21–L23; d) A. L. Balch, R. R. Guimerans, M. M. Olmstead, *J. Organomet. Chem.* **1984**, *268*, C38–C42; e) A. L. Balch, M. M. Olmstead, *Isr. J. Chem.* **1985**, *25*, 189–195; f) A. L. Balch, L. A. Fossett, R. R. Guimerans, M. M. Olmstead, *Organometallics* **1985**, *4*, 781–788; g) A. L. Balch, J. C. Linehan, M. M. Olmstead, *Inorg. Chem.* **1985**, *24*, 3975–3976; h) A. L. Balch, L. A. Fossett, J. Linehan, M. M. Olmstead, *Organometallics* **1986**, *5*, 691–698; i) A. L. Balch, J. C. Linehan, M. M. Olmstead, *Inorg. Chem.* **1986**, *25*, 3937–3942; j) A. L. Balch, L. A. Fossett, M. M. Olmstead, *Organometallics* **1987**, *6*, 1827–1829; k) A. L. Balch, D. E. Oram, *J. Organomet. Chem.* **1988**, *349*, 245–256; l) A. L. Balch, L. A. Fossett, J. K. Nagle, M. M. Olmstead, *J. Am. Chem. Soc.* **1988**, *110*, 6732–6738.

[11] a) Y. Yamamoto, T. Tanase, H. Ukaji, M. Hasegawa, T. Igoshi, K. Yoshimura, *J. Organomet. Chem.* **1995**, *498*, C23–C26; b) T. Tanase, H. Ukaji, T. Igoshi, Y. Yamamoto, *Inorg. Chem.* **1996**, *35*, 4114–4119; c) T. Tanase, H. Ukaji, H. Takahata, H. Toda, T. Igoshi, Y. Yamamoto, *Organometallics* **1998**, *17*, 196–209; d) T. Tanase, M. Hamaguchi, R. A. Begum, S. Yano, Y. Yamamoto, *Chem. Commun.* **1999**, 745–746; e) T. Tanase, M. Hamaguchi, R. A. Begum, E. Goto, *Chem. Commun.* **2001**, 1072–1073; f) T. Tanase, E. Goto, R. A. Begum, M. Hamaguchi, S. Zhan, M. Iida, K. Sakai, *Organometallics* **2004**, *23*, 5975–5988; g) E. Goto, R. A. Begum, S. Zhan, T. Tanase, K. Tanigaki, K. Sakai, *Angew. Chem. Int. Ed.* **2004**, *43*, 5029–5032.

[12] Y. Takemura, H. Takenaka, T. Nakajima, T. Tanase, *Angew. Chem. Int. Ed.* **2009**, *48*, 2157–2161.

[13] Y. Takemura, T. Nakajima, T. Tanase, *Dalton Trans.*, in press.

[14] a) Effendy, C. D. Nicola, M. Nitiatmodjo, C. Pettinari, B. W. Skelton, A. H. White, *Inorg. Chim. Acta* **2005**, *358*, 735–747; b) H.-K. Yip, H.-M. Lin, K.-K. Cheung, C.-M. Che, Y. Wang, *Inorg. Chem.* **1994**, *33*, 1644–1651.

[15] a) R. Terroba, M. B. Hursthouse, M. Laguna, A. Mendia, *Polyhedron* **1999**, *18*, 807–810; b) M. Laguna, M. D. Villacampa, M. Contel, J. Garrido, *Inorg. Chem.* **1998**, *37*, 133–135.

[16] a) B. Djordjevic, O. Schuster, H. Schmidbaur, *Inorg. Chem.* **2005**, *44*, 673–676; b) J.-P. Zhang, Y.-B. Wang, X.-C. Huang, Y.-Y. Lin, X.-M. Chen, *Chem. Eur. J.* **2005**, *11*, 552–561.

[17] L. Lettko, J. S. Wood, M. D. Rausch, *Inorg. Chim. Acta* **2000**, *308*, 37–44.

[18] É. Fournier, F. Lebrun, M. Drouin, A. Decken, P. D. Harvey, *Inorg. Chem.* **2004**, *43*, 3127–3135.

[19] a) M. Drag, A. Jezierski, P. Kafarski, *Chem. Commun.* **2004**, 1132–1133; b) I. J. B. Lin, J. S. Lal, C. W. Liu, *Organometallics* **1990**, *9*, 530–531; c) A. Caballero, F. A. Jalón, B. R. Manzano, G. Espino, M. Pérez-Manrique, A. Mucientes, F. J. Poblete, M. Maestro, *Organometallics* **2004**, *23*, 5694–5706.

[20] H. M. Walborsky, G. E. Niznik, *J. Org. Chem.* **1972**, *37*, 187–190.

[21] *Crystal Clear, version 1.3.5*, Rigaku and Molecular Structure Corp., The Woodlands, Texas, USA, **2003**.

[22] P. T. Beurskens, G. Admiraal, G. Beurskens, W. P. Bosman, R. de Gelder, R. Israel, J. M. M. Smits, *DIRDIF94 Program System*, Technical Report of the Crystallography Laboratory, University of Nijmegen, The Netherlands, **1994**.

[23] a) A. Altomare, M. C. Burla, M. Camalli, M. Cascarano, C. Giacovazzo, A. Guagliardi, G. Polidori, *J. Appl. Crystallogr.* **1994**, *27*, 435; b) A. Altomare, M. Burla, M. Camalli, G. Cascarano, C. Giacovazzo, A. Guagliardi, A. Moliterni, G. Polidori, R. Spagna, *J. Appl. Crystallogr.* **1999**, *32*, 115–119.

[24] a) G. M. Sheldrick, *SHELXL97, Program for the Refinement of Crystal Structures*, University of Göttingen, Germany, **1997**; b) G. M. Sheldrick, *SHELXL93, Program for the Refinement of Crystal Structures*, University of Goettingen, Germany, **1993**.

[25] *teXan, Crystal Structure Analysis Package*, Molecular Structure Corporation, **1985**, **1999**.

[26] *Crystal Structure 3.7.0, Crystal Structure Analysis Package*, Rigaku and Rigaku/MSC, The Woodlands, Texas, USA, **2000–2005**.

Received: July 11, 2009